

APPLICATIONS OF A CONSTRAINED INVERSION AND AN EXTENDED KRIGING METHOD TO
IMPROVE SOURCE, PATH, AND SITE CORRECTIONS FOR REGIONAL SEISMIC PHASES

Mark D. Fisk¹ and Steven R. Taylor²

Alliant Techsystems¹ and Rocky Mountain Geophysics, LLC²

Sponsored by National Nuclear Security Administration

Contract No. DE-AC52-06NA27321

Proposal No. BAA06-19

ABSTRACT

Objectives of this project are to develop and apply two methods to improve source and path corrections for regional seismic phases. In the first, we estimate and constrain source parameters using Brune (1970) model fits to relative spectra of regional seismic phases for event pairs with similar locations and focal mechanisms, but different seismic moments. We then use the source-corrected spectra to estimate geometrical spreading, Q , and site terms for Pn, Pg, Sn, and Lg in Eurasia. This constrained approach eliminates a fundamental trade-off, thereby improving estimates of source and distance corrections. We performed a preliminary study using waveform cross-correlations from Dr. Schaff for events prior to 2000 in Eurasia to find suitable pairs. We extended the analysis to event pairs in Eurasia from 2000 to 2006. Using the Preliminary Determination of Epicenters (PDE) catalog, we formed a list of candidate pairs, acquired a very large volume of regional data from the Incorporated Research Institutions for Seismology (IRIS), and computed waveform cross-correlations to find pairs of similar events. We computed and fit network-median relative spectra for almost 3,600 pairs. We automated these processing steps and finished reviewing and refining the results. We merged these results with our previous ones to obtain more extensive estimates of source corner frequencies versus moment and stress-drop parameters for Eurasia. We generated kriged grids of stress drop and associated uncertainties. We further fit the combined distance and site terms to the source-corrected spectra, showing that robust estimates of these effects are possible by first constraining source terms. We describe further work to separately constrain Q , geometrical spreading, and site parameters.

The second method, an extension to Bayesian kriging, provides robust path corrections and uncertainties for regional phase amplitudes, that properly treats localized calibration events that may have anomalous, correlated amplitudes. Clusters of anomalous reference events can significantly bias kriged amplitude corrections and uncertainties, if this correlation is not treated. Fisk and Taylor (2007) demonstrated the problem for a cluster of Rock Valley earthquakes at the Nevada Test Site (NTS) that have very high Pn/Lg values, leading to miscategorization of some NTS explosions. To address this issue, Fisk and McCartor (2008) developed a fundamental improvement to the kriging methodology, incorporating an additional correlation length to treat similar focal mechanisms, and tested the method on the NTS datasets and on large samples of underground nuclear explosions (UNEs) and earthquakes worldwide. Application to the worldwide datasets indicates that the power of the hypothesis test to reject earthquakes as explosions is marginally reduced, without miscategorizing any known explosions and providing a robust treatment of clustered data.

Report Documentation Page

Form Approved
OMB No. 0704-0188

Public reporting burden for the collection of information is estimated to average 1 hour per response, including the time for reviewing instructions, searching existing data sources, gathering and maintaining the data needed, and completing and reviewing the collection of information. Send comments regarding this burden estimate or any other aspect of this collection of information, including suggestions for reducing this burden, to Washington Headquarters Services, Directorate for Information Operations and Reports, 1215 Jefferson Davis Highway, Suite 1204, Arlington VA 22202-4302. Respondents should be aware that notwithstanding any other provision of law, no person shall be subject to a penalty for failing to comply with a collection of information if it does not display a currently valid OMB control number.

1. REPORT DATE SEP 2008		2. REPORT TYPE		3. DATES COVERED 00-00-2008 to 00-00-2008	
4. TITLE AND SUBTITLE Applications of a Constrained Inversion and an Extended Kriging Method to Improve Source, Path, and Site Corections for Regional Seismic Phases				5a. CONTRACT NUMBER	
				5b. GRANT NUMBER	
				5c. PROGRAM ELEMENT NUMBER	
6. AUTHOR(S)				5d. PROJECT NUMBER	
				5e. TASK NUMBER	
				5f. WORK UNIT NUMBER	
7. PERFORMING ORGANIZATION NAME(S) AND ADDRESS(ES) Alliant Techsystems,7480 Flying Cloud Dr,Minneapolis,MN,55344				8. PERFORMING ORGANIZATION REPORT NUMBER	
9. SPONSORING/MONITORING AGENCY NAME(S) AND ADDRESS(ES)				10. SPONSOR/MONITOR'S ACRONYM(S)	
				11. SPONSOR/MONITOR'S REPORT NUMBER(S)	
12. DISTRIBUTION/AVAILABILITY STATEMENT Approved for public release; distribution unlimited					
13. SUPPLEMENTARY NOTES Proceedings of the 30th Monitoring Research Review: Ground-Based Nuclear Explosion Monitoring Technologies, 23-25 Sep 2008, Portsmouth, VA sponsored by the National Nuclear Security Administration (NNSA) and the Air Force Research Laboratory (AFRL)					
14. ABSTRACT see report					
15. SUBJECT TERMS					
16. SECURITY CLASSIFICATION OF:			17. LIMITATION OF ABSTRACT	18. NUMBER OF PAGES	19a. NAME OF RESPONSIBLE PERSON
a. REPORT unclassified	b. ABSTRACT unclassified	c. THIS PAGE unclassified			

OBJECTIVES

We have been developing and testing two methods to improve magnitude and path corrections for regional seismic phase amplitudes. Objectives of the first method, a constrained inversion approach, are to improve estimates of geometrical spreading and Q models for Pn, Pg, Sn, Lg in Eurasia, by eliminating trade-offs with source corner frequencies, and to improve source parametrizations in Eurasia, in terms of grids of stress drop and corner frequency scaling. The objective of the second method, an extension to Bayesian kriging, is to provide robust path-specific corrections and uncertainties for regional phase amplitudes, that properly treat localized calibration events that may have anomalous, correlated amplitudes. This project has three main tasks: (Task 1) Assemble multiple datasets of regional seismic recordings of earthquakes throughout broad areas of Eurasia; apply waveform cross-correlation techniques to determine nearby pairs/clusters of events; and assemble spectral amplitude measurements of Pn, Pg, Sn, and Lg for the events. (Task 2) Implement a technique to estimate corner frequencies and scaling parameters by fitting relative spectra of a Brune model to data for pairs of nearby earthquakes of different moments; compute grids of stress drop and earthquake corner-frequency scaling with moment for Eurasia; use spectral amplitude data for regional phases and constrained source parametrizations to perform a robust inversion for geometrical spreading and Q-model parameters; and test and evaluate resulting magnitude and distance corrections on events in Eurasia, using cross-validation methods. (Task 3) Investigate clusters of earthquakes to assess the potential for events with anomalous, correlated mechanisms to bias kriged amplitude correction grids beyond existing uncertainty estimates; develop a technique to quantify the correlation of regional phase amplitudes within clusters; extend a Bayesian kriging method to incorporate these correlation measures in the computation of amplitude correction and uncertainty grids; and test and evaluate the methods on events in Eurasia, using cross-validation techniques. We plan to deliver the techniques, parametrizations of stress drop, corner frequency scaling, geometrical spreading and Q models, and kriged amplitude correction and uncertainty grids for stations in Eurasia.

RESEARCH ACCOMPLISHED

Constrained Inversion Technique

We have implemented and applied an approach to constrain the source parameters for earthquakes throughout Eurasia, using Brune (1970) model fits to relative spectra of regional phases for nearby event pairs/clusters with similar mechanisms, but different seismic moments. We assembled and processed very large datasets for this effort. We have further estimated fits of the combined distance and site terms, which show that robust estimates of these effects may now be obtained by first constraining and removing the source scaling. Following Sereno et al. (1988) and Taylor and Hartse (1998), the amplitude spectrum for a given phase and station, for event i , may be modeled by

$$A_i(f) = S_i(f, f_c) G(r_i, r_0) \exp\left(-\frac{\pi f}{Q(f)v} r_i\right) P(f), \quad (\text{EQ 1})$$

where $S_i(f, f_c)$ is the source spectrum with corner frequency f_c , r_i is the epicentral distance, v is the group velocity, $P(f)$ is the site term, $Q(f) = Q_0 f^\eta$ is the frequency-dependent attenuation, $G(r, r_0)$ is the frequency-independent geometrical spreading, taken to be inversely proportional to distance to a power η , beyond a reference distance r_0 . Taylor et al. (2002) and others have used the logarithm of Equation (1) in a grid search to simultaneously estimate all of the parameters. However, significant trade-offs among the parameter estimates are well known and difficult to constrain by standard techniques and available data (e.g., Taylor and Hartse, 1998). This has led to grossly inaccurate corrections of regional amplitudes for distance and magnitude. Fisk and Taylor (2006) discuss examples.

Instead of performing a grid search for all parameters simultaneously, we use relative spectra for event pairs with similar locations and focal mechanisms (assessed by waveform cross-correlations), but different moments, to factor

out path and station effects and obtain reliable estimates of the source parameters. That is, for a pair of nearby earthquakes with similar radiation patterns, the model relative spectra for a given phase type is given by

$$\frac{A_1(f)}{A_2(f)} = \frac{S_1(f)}{S_2(f)} = \frac{M_0^{(1)}[1 + (f/f_c^{(2)})^2]}{M_0^{(2)}[1 + (f/f_c^{(1)})^2]} \quad (\text{EQ 2})$$

For a Brune (1970) dislocation source, the corner frequency for seismic phase type ξ is given by

$$f_c(\xi) = c_\xi v_s(\xi) \left(\frac{\sigma_b}{M_0} \right)^{1/3}, \quad (\text{EQ 3})$$

where σ_b is the stress drop, $v_s(\xi)$ is the source medium velocity for P or S waves, and c_ξ is a constant that can depend on phase type. Walter and Taylor (2002) allow for non-constant stress drop by defining the apparent stress drop for a given seismic moment, M_0 , as

$$\sigma_b = \sigma_b^{(0)} \left(\frac{M_0}{M_0^{(0)}} \right)^\psi, \quad (\text{EQ 4})$$

where $\sigma_b^{(0)}$ is the stress drop at reference moment $M_0^{(0)}$. Using pairs of localized earthquakes, we fit $\sigma_b^{(0)}$ and ψ to empirical relative spectra of regional phases. Figure 1 illustrates the network-averaged relative spectra and model fits for an earthquake pair in Kyrgyzstan during 1997. The relative spectra are quite similar for the various phases, although over different frequency ranges because of phase-dependent signal-to-noise limitations. Hence, the model fits, and estimated corner frequencies are very similar. This appears to be a fairly common and important phenomenon for the earthquakes analyzed.

Using waveform cross-correlations for 4,236 events in Eurasia prior to 2000 (*cf.* Schaff and Richards, 2004) to find a subset of event pairs in the Los Alamos National Laboratory (LANL) database, we acquired seismograms from IRIS, added and refined regional phase picks, computed the spectra, averaged relative spectra over stations, and fit the model for each phase, and for all available phases simultaneously, as in Figure 1. We allowed the relative moments to be estimated from the relative spectra or to use moment magnitudes (M_W) from LANL. We performed three types of fits in which the apparent stress-drop scaling parameter, ψ , is a free parameter or fixed at 0.0 or 0.25. The latter two cases correspond, respectively, to corner frequency scaling as

$M_0^{-1/3}$ (Brune, 1970) or as $M_0^{-1/4}$ (Nuttli, 1983; Cong et al., 1996; Walter and Taylor, 2002). We computed kriged grids of stress drop for these three cases.

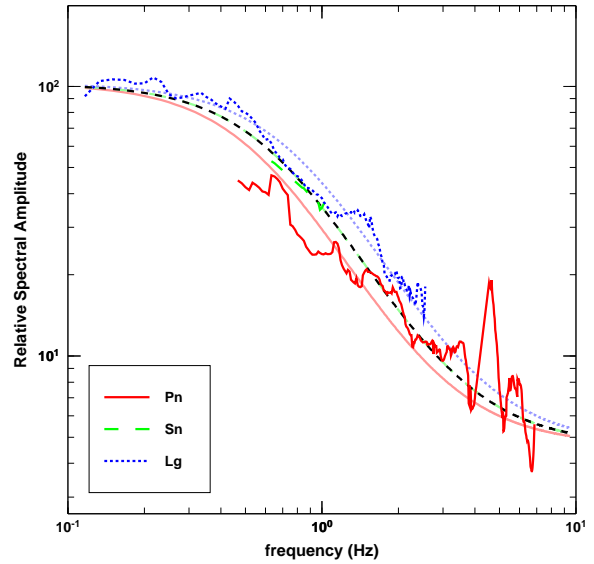


Figure 1. Example of relative spectra for a pair of M_W 6.0 and 4.7 earthquakes in Kyrgyzstan. Model fits for each phase are represented by corresponding line types. The black dashed curve shows the model fit using relative spectra for all available phases.

Figure 2 shows corner frequency estimates versus log moment for Pn, Sn, and Lg for events in Eurasia, fixing $\psi = 0$ in this case. Linear fits are shown with (dashed) and without (solid) the slopes fixed at $-1/3$. Considering the amount of scatter due to spatial and other variations, the fits are remarkably consistent for all phases, and the slope estimates are all close to -0.33 , although the slope estimates depend on the explicit treatment of ψ .

Figure 3 shows that Pn and Lg corner frequencies are fairly similar for most of the earthquakes in diverse areas of Eurasia, comparable to findings by Walter and Taylor (2002) for western U.S. earthquakes. This is important for two reasons. First, it helps explain why P/S ratios discriminate more effectively at higher frequencies, in most areas examined (provided path and station effects are properly treated). That is, as shown by Fisk (2006, 2007) the frequency dependence of P/S discrimination performance depends on the ratio of P- and S-wave corner frequencies squared. This ratio is significantly larger for explosions than earthquakes at all sites examined. Thus, P/S ratios exhibit less frequency

dependence for earthquakes than explosions. Second, this result allows more robust fitting of Brune source parameters, using a broader range of frequencies, by combining relative spectra of regional P and S phases for earthquakes (e.g., the black dashed curve in Figure 1).

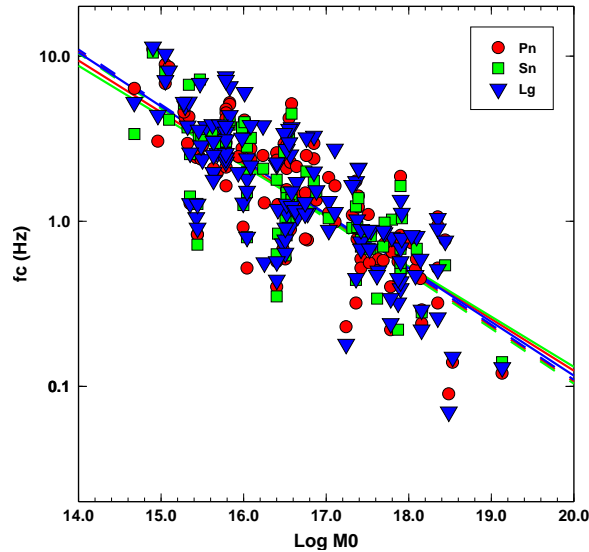


Figure 2. Corner frequency estimates of Pn, Sn, and Lg spectra versus log moment for events in Eurasia. Linear regression fits (lines) are shown, indicating scaling with source size.

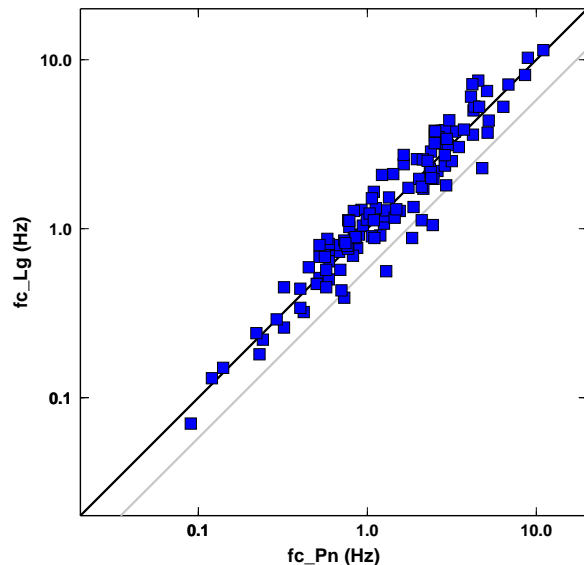


Figure 3. Estimated Lg versus Pn corner frequencies, indicating similar values for most of the earthquakes. Black and gray lines represent ratios of 1.0 and 1.73 (cf. Madariaga, 1976; Choy and Boatwright, 1995).

Figure 4 shows preliminary kriged stress-drop grids based on Lg (left) and Pn (right) data. The grids are very similar, indicating similar stress-drop estimates from Lg and Pn. There are concerns that stress-drop estimates by other approaches are biased due to trade-offs with Q (e.g., Phillips et al., 2008, discuss stress drop bias in low Q regions). Such bias is not present in our analysis because we use relative spectra that factor out Q effects.

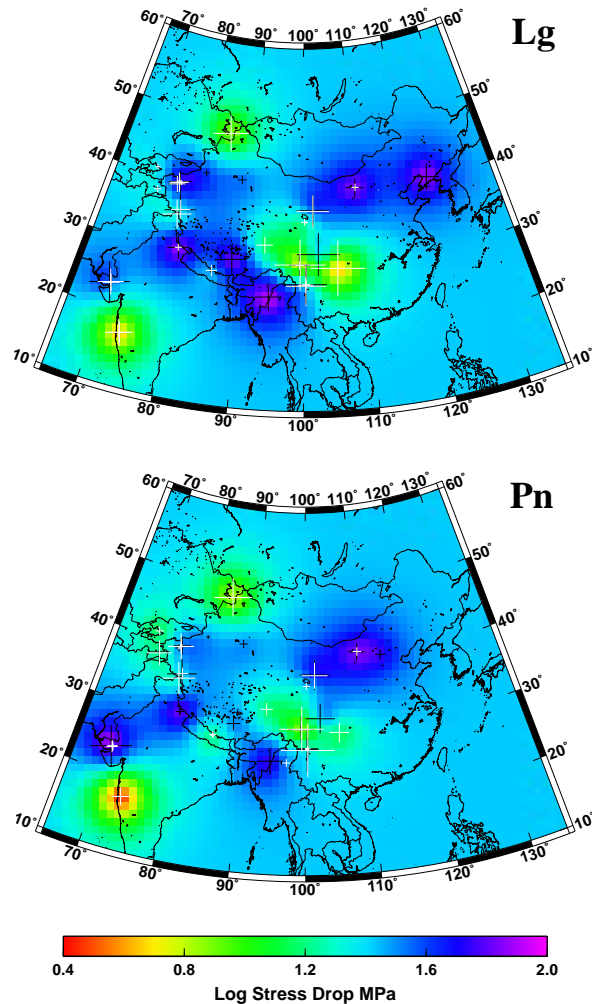


Figure 4. Initial kriged grids of stress drop based on estimates from Lg (top) and Pn (bottom) relative spectra. The size and color of the markers indicate the absolute residual and sign relative to the grid.

We extended our analysis of relative spectra to event pairs in Eurasia from 2000 to 2006 (see Figure 5). Using the PDE catalog, we formed a list of candidate pairs, based on proximity and relative mb or M_w values in the PDE, and acquired a very large volume of regional data

from the IRIS Data Management Center (DMC) for the events. We then computed waveform cross-correlations to find similar event pairs, like the analysis by Schaff and Richards (2004). We computed and fit network-median relative spectra for almost 3600 pairs of events. We have automated all of these processing steps, although it is still necessary to review and refine the results. In the Brune model-fitting analysis, we fix the moment of the larger event of the pair (in the numerator), assuming it is better recorded and, hence, has a more reliable moment estimate. We then estimate the moment of the smaller event, based on the network-median relative spectra.

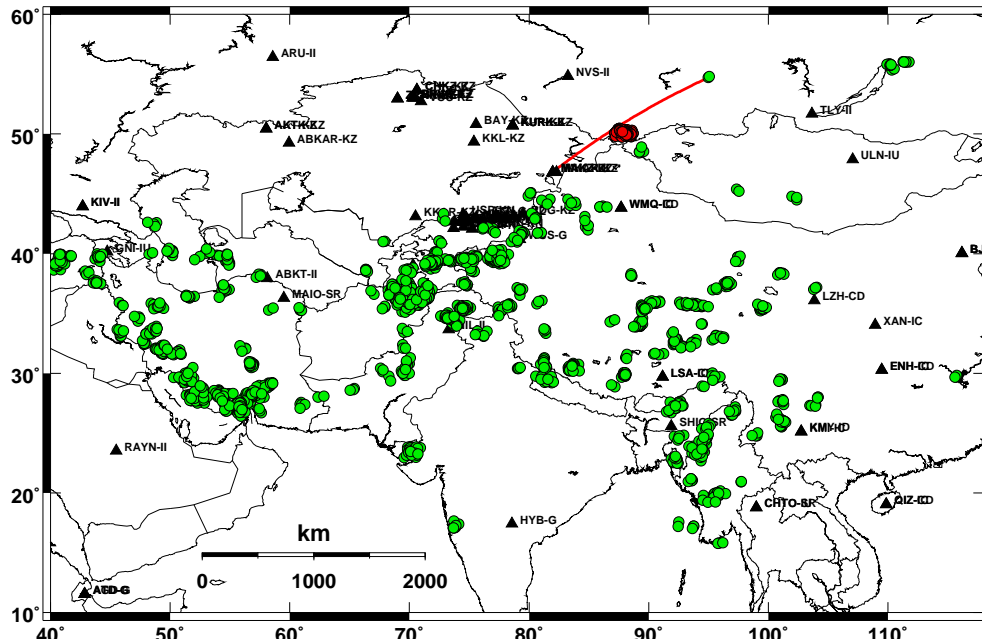


Figure 5. Events and stations used to process relative spectra and fit corner frequencies and stress drops. The cluster highlighted in red and the great-circle path along two clusters to MAKZ are discussed below.

We have finished reviewing and refining the automatic processing and Brune model-fitting results, completing a major and important quality control (QC) effort. Figure 6 shows an example for one event pair associated with the highlighted cluster in Figure 5. Figure 7 shows the corner frequency estimates for all pairwise combinations using three large master events (circles, diamonds, and squares), the median value for each event (triangles), and the scaling relation with log moment (line) for this cluster. These plots indicate the degree to which the source parameters may be constrained by our approach. We have merged these results with our previous results (that were processed purely manually, including phase picks, spectral processing, network averaging, and model fitting) to obtain more extensive estimates of corner frequencies versus moment and stress-drop parameters for Eurasia. We have generated kriged grids of stress drop and the associated uncertainties for Eurasia (Figure 8).

We have used the estimated Brune source terms (corner frequencies and stress drops) to correct the spectra for source scaling. We generally find that the source-corrected spectra are quite similar for events in a given cluster, indicating that the source corrections are very consistent, based on our Brune model fitting of the relative spectra. Using these instrument- and source-corrected spectra, we have estimated the combined effects of Q, geometrical spreading, and site effects. Under the standard model of Equation (1), geometrical spreading is a constant (i.e., independent of frequency) for a cluster at a fixed distance from a given station. This allows the frequency-dependent Q and site terms to be fit to the corrected log spectra versus log frequency. The constant of this fit involves geometrical spreading and a constant site factor. We use the median of the corrected spectra for a given cluster/station, which is more robust to outliers than the average. Results of these fits to various clusters have been very encouraging.

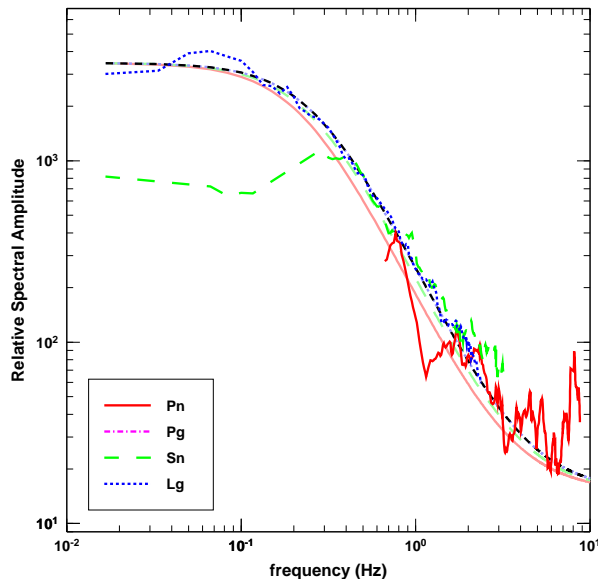


Figure 6. Network-median relative spectra of Pn, Sn, and Lg for a pair of events in the cluster depicted by red markers in Figure 5. Also shown are the Brune relative source model fits (smooth curves).

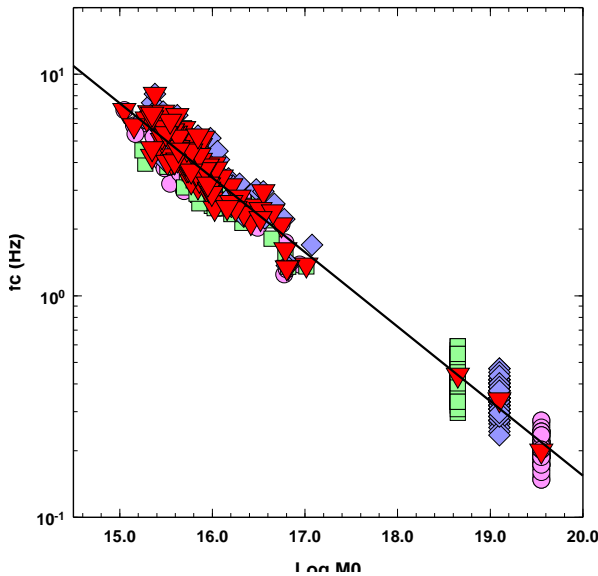


Figure 7. Corner frequency versus log moment for the cluster highlighted by red markers in Figure 5, estimated by fitting the combined relative spectra of Pn, Sn, and Lg, as in Figure 6. Shown are estimates for all pairwise combinations using three large master events (circles, diamonds, squares), the median value for each event (triangles), and the scaling relation with log moment (line) for this cluster.

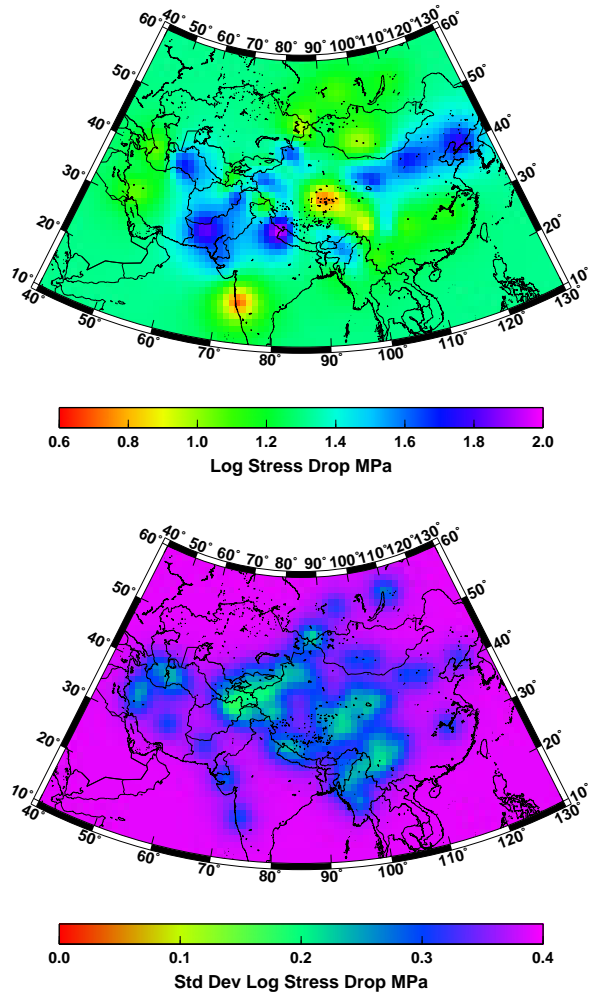


Figure 8. Updated kriged grids of stress drop (top) and calibration standard deviation (bottom) using combined relative spectra of Pn, Sn, and Lg and merging our initial and recent processing results.

For example, Figure 9 shows the source-corrected Lg spectra at BRVK (Borovoye, Kazakhstan) for the cluster depicted by red circles in Figure 5. It illustrates several important aspects of our analysis. First, the light blue curves show the corrected Lg spectra for each event that was recorded by BRVK. Overall, the curves are fairly similar in shape and relative amplitude offset, indicating that the corrections for source terms (moments and corner frequencies) are effective and consistent. There are modest departures at low and high frequencies, where noise effects bias the spectra. Second, the median corrected Lg spectrum (red curve) for the cluster is robust to outliers. For example, the lowest blue curve is

due to a bad BRVK BHZ recording that slipped through the automated QC criteria. Although such cases are rare, they can significantly impact the mean, if used instead of the median. Third, the fit (black curve) to the median spectrum illustrates very good agreement over a wide range of frequencies. We have generated comparable results for all of the recording stations and for other clusters (i.e., paths) with various numbers of events.

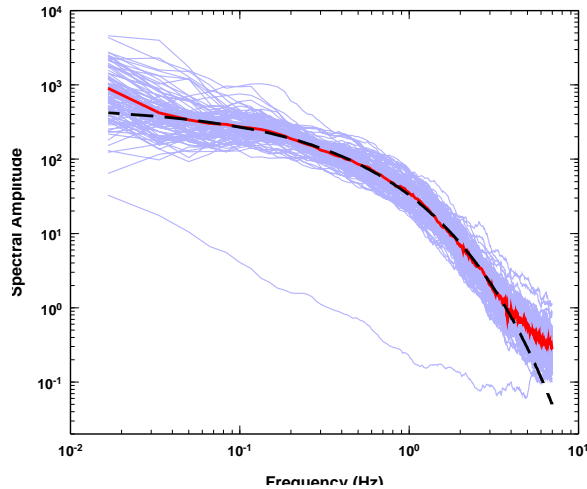


Figure 9. Source-corrected Lg spectra at BRVK for all events in the cluster (blue), the median (red), and a model fit of the combined distance and site effects (black dashed).

The black dashed curve provides excellent calibration over a wide range of frequencies for all of the combined non-source-related physical effects (Q , spreading, and site terms) for this path/station. For an isolated cluster, these fits do not provide independent, reliable estimates of the individual path and site parameters. For example, to estimate accurate Q parameters (Q_0 and γ), we need to separate their frequency dependence from that of the site term. One option is to use all available source-corrected spectra to perform a large inversion for these remaining parameters. This will give distinct parameter estimates but, based on experience, these quantities will still have trade-offs that are not well constrained.

We have also been investigating alternative, more innovative analyses to constrain the remaining trade-offs and separate the path and site effects that do and do not depend on frequency and distance. Separating these terms is important and beneficial for several reasons. First, it allows physical interpretation and comparison of

estimated model parameters to other results. Second, it allows more reliable interpolation of spatially-varying physical parameters (e.g., Q_0). Third, it allows merging results we obtain with existing models at LANL. Note that the constant term of the model fit to the source-corrected spectrum (e.g., the offset of the black curve in Figure 9) depend only on geometrical spreading and a constant site term. Since the former term depends on distance and the latter does not, we can use the constants of the fits for all clusters/pairs of events recorded by a given station at different distances to separately constrain them. Once we estimate these terms, the only remaining parameters to be resolved are Q_0 , γ , and one that governs the frequency dependence of the site term. We have investigated various approaches for this final step. One is to insert the spectra for all of the events in our datasets, now corrected for all but these two terms, into a grid search for three parameters. This is a much smaller parameter space than the full space associated with Equation (1). As in separating the spreading and constant site terms, Q_0 and γ can be separated from the frequency-dependent site term by distance.

Another approach that imposes an additional constraint on these last 3 parameters is to use the relative median spectra for clusters with similar paths, but at different distances from a station, to factor out the site term and obtain a robust estimate of Q for that path. This estimate of Q has no trade-off with source, site, or geometrical spreading effects. Figure 10 illustrates this approach. It shows the ratio of the median spectra at station MAKZ (Makanchi, Kazakhstan), already corrected for source terms, for the two clusters along the great-circle path in Figure 5. This relative spectrum factors out the site term. The geometrical spreading terms for these two clusters are different constants, i.e., independent of frequency. Mathematically, assuming Q is relatively constant over a path, the ratio of source-corrected, median spectra for the two clusters is simply given by

$$\log(\bar{A}_1/\bar{A}_2) = \frac{\pi f^{1-\gamma}}{Q_0 v} \Delta r, \quad (\text{EQ 5})$$

where Δr is the separation of the clusters. Fitting this expression to empirical spectral ratios gives constrained estimates of Q_0 and γ (e.g., Lg $Q_0 = 546$ for the path depicted in Figure 5 and associated with Figure 10).

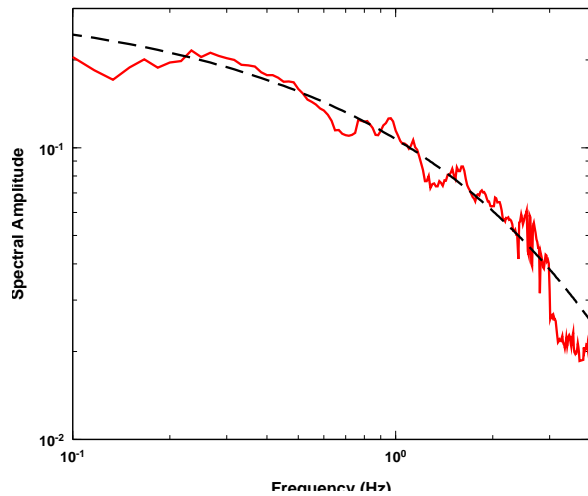


Figure 10. Ratio of source-corrected median spectra at MAKZ for two clusters along the great-circle path in Figure 5. The relative spectrum factors out the site term and allows a robust estimate of Q for this path.

Correcting the source-corrected spectra of these clusters now for Q , the remaining frequency dependence is due to site effects. Once this is done for at least one path, the frequency-dependent site term may be estimated and fixed, under the assumption of the standard model that $P(f)$ is independent of azimuth. We can then estimate Q for all paths with available data. The other assumption is that a suitable path exists for a given station along which Q is fairly constant. We need to investigate its validity for stations of interest. Although this research would require some effort, the potential payoff is substantial to constrain and improve Q models in Eurasia. We refer to the overall approach as a stepwise, iterative procedure to constrain all of the parameters of the standard model, using our available source-corrected spectra and preliminary model fits (as in Figure 9) as a starting point.

Treatment of Correlation for Clustered Reference Data in Kriging Regional Seismic Discriminants

As a separate study, we also investigated the effects of anomalous regional phase amplitudes (from events with abnormal mechanisms, depths, and/or paths) on kriged amplitude corrections and uncertainties, and the impact on discrimination errors. We demonstrated the problem using a cluster of Rock Valley (RV) earthquakes at NTS that have very high Pn/Lg values. In the worst case,

using only RV earthquakes to calibrate station KNB, 11 of 88 NTS UNEs are miscategorized as *earthquake-like*. The reason for this error rate is that the RV events have very high Pn/Lg values at KNB (2.6σ above the global average), biasing the kriged corrections at NTS, and the posterior calibration uncertainty computed by the old kriging method (Bottone et al., 2002) is small, treating the 11 RV events as independent. Since all of the RV events have similar mechanisms (Smith and Brune, 1993) and highly correlated waveforms (e.g., Figure 11), it is invalid to treat their Pn/Lg values as independent in the kriging analysis.

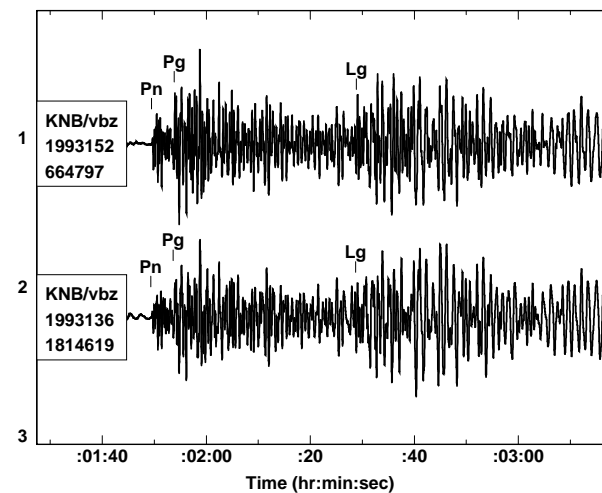


Figure 11. Seismic recordings (0.5–5.0 Hz) of two RV events by KNB, showing their similarity.

To ameliorate this problem, Fisk and McCartor (2008) extended the Bayesian kriging method of Bottone et al. (2002), incorporating an additional correlation length. The original correlation length treats regional path variations, estimated to be about 5 to 6 degrees for Pn/Lg and Pn/Sn in various region types (Bottone et al., 2002). The new correlation length treats events with similar focal mechanisms that typically occur on much shorter distance scales of faulting zones (e.g., a few km for the RV events). Treating this correlation limits the effective number of reference data for clustered events. It keeps the corrections from weighting such data too heavily and the posterior calibration variance from being too small. Fisk and McCartor (2008) showed that no NTS UNEs are miscategorized by the new method, even replicating the entire set of RV events 20 times. Many events are *undetermined* by the new procedure for the KNB/RV

case, but this is appropriate, given the very anomalous RV reference data. Fortunately, such cases are rare (i.e., less than 1% for values 2.6σ above the global average). The fact that a large fraction of events are *undetermined* for rare and anomalous cases should not be alarming. In fact, application to global datasets shows that the power of the test to reject earthquakes as being explosions at the 99.5% confidence level did not degrade much from the original screening rate of 78%, even for relatively large values of the new correlation length, α_r (Figure 12).

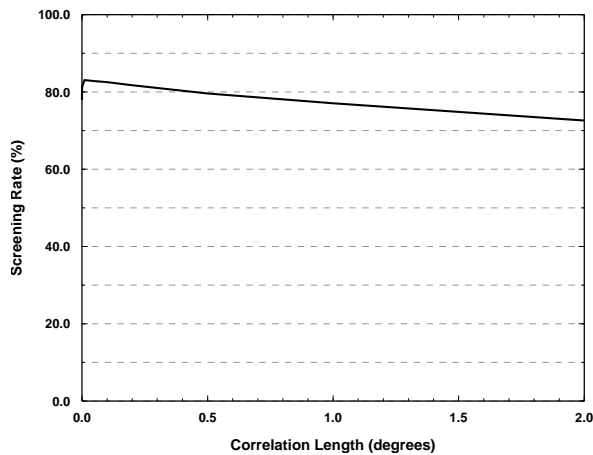


Figure 12. Percentage of earthquakes worldwide that are rejected as *explosion-like* at the 0.005 significance level as a function of the correlation length α_r .

CONCLUSIONS AND RECOMMENDATIONS

We developed and tested two methods to improve source and path corrections for regional seismic phases. The first estimates and constrains source parameters using Brune model fits to relative spectra of regional phases for event pairs with similar mechanisms, but different moments. We applied it to two very large datasets in Eurasia. We automated the various processing steps, including assessment of event pairs from waveform cross-correlations, computing network-median of relative spectra (large over small events), and fitting the Brune model to estimate corner frequencies and stress drop. We used kriging to compute grids of stress drop for Eurasia. Using spectra corrected for source terms, we have fit the combined distance and site effects for the various events and stations in our dataset, showing that good calibration of non-source-related physical effects

(distance and site terms) may be obtained over a wide range of frequencies for paths with data.

We also investigated ways to constrain remaining trade-offs among Q, geometrical spreading, and site terms that have different dependencies on distance and frequency. We advocate a stepwise, iterative procedure to constrain all parameters of the standard model. Starting with our source-corrected spectra and the model fits (e.g., shown in Figure 9), the procedure would separate the spreading and constant site terms, apply those corrections, and then resolve Q and frequency-dependent site terms. This is expected to provide more accurate estimates of all of the physical parameters of Equation (1) than currently exist. In the future, we would also like to incorporate coda measurements and methods (1) to augment the source terms estimated using spectra of direct phases, relaxing the restriction on event pairs with similar mechanisms; and (2) as a way to independently estimate site terms.

Second, we extended the Bayesian kriging method of Bottone et al. (2002), introducing a second correlation length to treat clusters of correlated reference events. This limits the effective number of samples for such clusters. We have shown that the new method does not miscategorize any NTS UNEs, even replicating the set of RV events many times. Thus, the extended method is very robust. Although many events were *undetermined* for this case, this is appropriate for the anomalous RV reference data. Fortunately, such cases are rare. In fact, application to global datasets shows that the power of the test to reject earthquakes as explosions does not degrade much, even for fairly large values of α_r . Thus, a practical solution is available, using a conservative value of α_r , with little impact on overall performance. This is also encouraging because location estimates in most realistic situations may not have sufficient precision to allow use of smaller values of α_r . Further work is needed to estimate α_r . Although this does not seem necessary for the global case, application to specific sites may improve significantly by using site-specific values. Treatment should include how the data are explicitly correlated, especially for areas where various numbers of clusters with distinct mechanisms occur, e.g., in terms of correlations of waveforms or amplitude data.

ACKNOWLEDGMENTS

We thank Gary McCartor and Steve Bottone for many useful discussions, Bill Walter and Ward Hawkins for providing seismic data, and David Schaff for providing waveform cross-correlation values. We acknowledge the IRIS DMC for seismic data used in this study.

REFERENCES

- Bottone, S., M. D. Fisk and G. D. McCartor (2002). Regional seismic event characterization using a Bayesian formulation of simple kriging, *Bull. Seism. Soc. Am.* 92: 2277–2296.
- Brune, J. N. (1970). Tectonic stress and the spectra of seismic shear waves from earthquakes, *J. Geophys. Res.* 75: 4997–5009.
- Choy, G. L. and J. L. Boatwright (1995). Global patterns of radiated seismic energy and apparent stress, *J. Geophys. Res.* 100: 18,205–18,228.
- Cong, L., J. Xie and B. J. Mitchell (1996). Excitation and propagation of Lg from earthquakes in central Asia with implications for explosion/earthquake discrimination, *J. Geophys. Res.* 101: 27,779–27,789.
- Fisk, M. D. (2007). Corner frequency scaling of regional seismic phases for underground nuclear explosions at the Nevada Test Site, *Bull. Seism. Soc. Am.* 97: 977–988.
- Fisk, M. D. (2006). Source spectral modeling of regional P/S discriminants at nuclear test sites in China and the Former Soviet Union, *Bull. Seism. Soc. Am.* 96: 2348–2367.
- Fisk, M. D. and G. D. McCartor (2008). Treatment of correlation for clustered reference data in kriging regional seismic discriminants, *Bull. Seism. Soc. Am.* 98: in press.
- Fisk, M. D. and S. R. Taylor (2006). Robust magnitude and path corrections for regional seismic phases in Eurasia by constrained inversion and enhanced kriging techniques, in *Proceedings of the 28th Seismic Research Review: Ground-Based Nuclear Explosion Monitoring*, LA-UR-06-5471, Vol. 1, pp. 15–24.
- Fisk, M. D. and S. R. Taylor (2007). Robust magnitude and path corrections for regional seismic phases in Eurasia by constrained inversion and enhanced kriging techniques, in *Proceedings of the 29th Monitoring Research Review: Ground-Based Nuclear Explosion Monitoring*, LA-UR-07-5613, Vol. 1, pp. 24–33.
- Madariaga, R. (1976). Dynamics of an expanding circular fault, *Bull. Seism. Soc. Am.* 66: 639–667.
- Nuttli, O. W. (1983). Average seismic source-parameter relations for mid-plate earthquakes, *Bull. Seism. Soc. Am.* 73: 519–535.
- Phillips, W. S., R. J. Stead, G. E. Randall, H. E. Hartse and K. Mayeda (2008). Source effects from broad area network calibration of regional distance coda waves, in *Scattering of Short Period Waves in the Heterogeneous Earth*, H. Sato and M. C. Fehler, Editors, in press.
- Schaff, D. P. and P. G. Richards (2004). Repeating seismic events in China, *Science* 303: 1176–1178.
- Sereno T. J., S. R. Bratt and T. C. Bache (1988). Simultaneous inversion of regional wave spectra for attenuation and seismic moment in Scandinavia, *J. Geophys. Res.* 93: 2019–2035.
- Smith, K. D. and J. N. Brune (1993). A sequence of very shallow earthquakes in the Rock Valley fault zone; southern Nevada test site, *EOS Suppl.* 74: 417.
- Taylor, S. R., and H. E. Hartse (1998). A procedure for estimation of source and propagation amplitude corrections for regional seismic discriminants, *J. Geophys. Res.* 103: 2781–2789.
- Taylor, S. R., A. A. Velasco, H. E. Hartse, W. S. Phillips, W. R. Walter, and A. J. Rodgers (2002). Amplitude corrections for regional seismic discriminants, *Pure and Appl. Geophys., Special Edition on Monitoring the Comprehensive Nuclear-Test-Ban Treaty: Seismic Event Discrimination and Identification* 159: 623–650.
- Walter, W. R., K. M. Mayeda, and H. J. Patton (1995). Phase and spectral ratio discrimination between NTS earthquakes and explosions. Part I: Empirical observations, *Bull. Seism. Soc. Am.* 85: 1050–1067.
- Walter, W. R. and S. R. Taylor (2002). A Revised Magnitude and Distance Amplitude Correction (MDAC2) Procedure for Regional Seismic Discriminants: Theory and Testing at NTS, UCRL-ID-146882, LA-UR-02-1008.